Shear Behaviour of Sand Under Generalized Conditions of Stress and Strain

by

P.C. Rawat*

T. Ramamurthy**

Introduction

IT has long been felt that if rapid progress is to be made in designing and predicting the performance of increasingly complicated soil structures, more emphasis should be given to the stress-strain behaviour of soils under conditions operating in the field. No account is taken of the deformation characteristics of soils in solving problems which are essentially deformational ones. Axisymmetric stress conditions ($\sigma_1' > \sigma_2' = \sigma_3'$, or, $\sigma_1' = \sigma_2' > \sigma_3'$) rarely occur and many field problems fall into the category of plane strain in which no deformation takes place in the direction of the intermediate principal stress. The importance of using parameters in the calculations which are appropriate to the particular deformation modes and stress paths undergone by elements of soil in the model or prototype have been often stressed (Smith and Kay, 1971). The appropriate parameters so obtained can be confidently used in solving a number of geotechnical problems employing finite element method of analysis. Thus, predictions can be made to a greater degree of accuracy.

Recognizing the importance of simulating field loading conditions in the laboratory, the recent research work (after 1965) has resulted in developing number of equipments in which principal stresses and strains acting on a prismatic soil sample can be independently controlled and measured employing various combinations of flexible and rigid boundaries. These equipments can be categorized into three groups based on the ways of applying normal boundary stresses :

(*a*) those employing rigid platens (Hambly, 1969; Pearce, 1971; Gudehus, 1971)

(*b*) those employing flexible rubber bags (Ko, 1966; Ko and Scott, 1967; Lomize and Kryzhanovsky, 1967; Lomize *et al*, 1969; Arthur and Menzies, 1968, 1972; Menzies, 1970, 1971; Lewin, 1971)

(*c*) those employing a combination of flexible and rigid boundaries (Shibata and Karube, 1965; Lenoe, 1966; Young and KcKyes, 1967,

---

* Soil Engineer, Ocean Engineering Division, Engineers India Ltd., Hindustan Times House, New Delhi-110001, India.

** Professor, Civil Engineering Department, Indian Institute of Technology, New Delhi-110029, India.

This paper was received in May 1978 and open for discussion till the end of January, 1979

1971; Bishop, 1967; Green, 1969, 1971*a*, *b*; Green and Bishop, 1969; Proctor and Barden, 1969; Mesdary, 1969; Sutherland and Mesdary, 1969; Mesdary and Sutherland, 1970; Bennet, 1969, 1971; Dyson, 1970; Ramamurthy, 1970; Sutherland, 1971; Barden and Proctor, 1971; Ramamurthy and Rawat, 1971, 1973; Reades, 1972; Lade and Duncan, 1973; Green and Reades, 1975; Reades and Green, 1976; Somashekar, 1977).

The advantages and disadvantages of these equipments have been discussed elsewhere (Mesdary, 1969; Reades, 1972; Rawat, 1976).

In the present paper, the design and performance of a modified Universal triaxial apparatus (originally developed by Ramamurthy, 1970) is described. This apparatus employs a combination of flexible and rigid boundaries to subject a 7.6 cm cubical soil specimen to three different and uniform direct stresses, and to permit measurement and control of strains. Results of consolidated drained shear tests conducted in this apparatus on cubical specimens of Ottawa sand under various combinations of major, intermediate, and minor principal stresses employing different stress paths are presented. Results of tests conducted in plane strain condition are also presented. The results of compression tests conducted in the modified universal triaxial apparatus (UTA) under axisymmetric conditions are compared with those obtained from the conventional triaxial apparatus (CTA) with regard to peak strength and stress-strain behaviour prior to peak.

Tests were also conducted on samples of glass ballotini. The results were found to be of similar nature as those from tests on Ottawa sand and are, therefore, not presented here.

General Description of Universal Triaxial Apparatus

Sectional plan and elevation of the modified UTA, and a photograph are shown in Figures 1 and 2 respectively. A 7.6 cm cubical specimen enclosed in a rubber membrane and sealed at the enlarged, rigid, lubricated platens is loaded axially in a constant rate of displacement triaxial loading frame. The axial load is measured with a proving ring which is in direct contact with the top platen. Flexible lubricated rubber bags filled with water and confined in metallic guides are used to apply lateral stresses on the other two pairs of faces. The rubber bags on the opposite faces are interconnected through a T-connection leading to a self-compensating mercury control system (Bishop and Henkel 1962). Two separate Bourdon pressure gauges are used to read applied lateral stresses. When one of the lateral stresses is higher than the other, the vertical edges of the bags applying the higher stress are reinforced with sponge prismatic pieces to prevent interference with the adjacent bags, and to avoid distortion of the vertical edges of the specimen. The deformation of the specimen in the vertical direction is recorded with a dial gauge (0.025 mm) attached to the bottom of the proving ring with extended spindle resting on the base platen which in turn is supported by the platform of the loading machine. The horizontal displacement of the mid-point of each vertical face of the specimen is transferred by means of a rod (attached to a stud embedded in the rubber bags from inside) passing through the metallic guide and is recorded with a dial gauge (0.025 mm). Four similar dial gauges record the lateral deformation of the specimen.

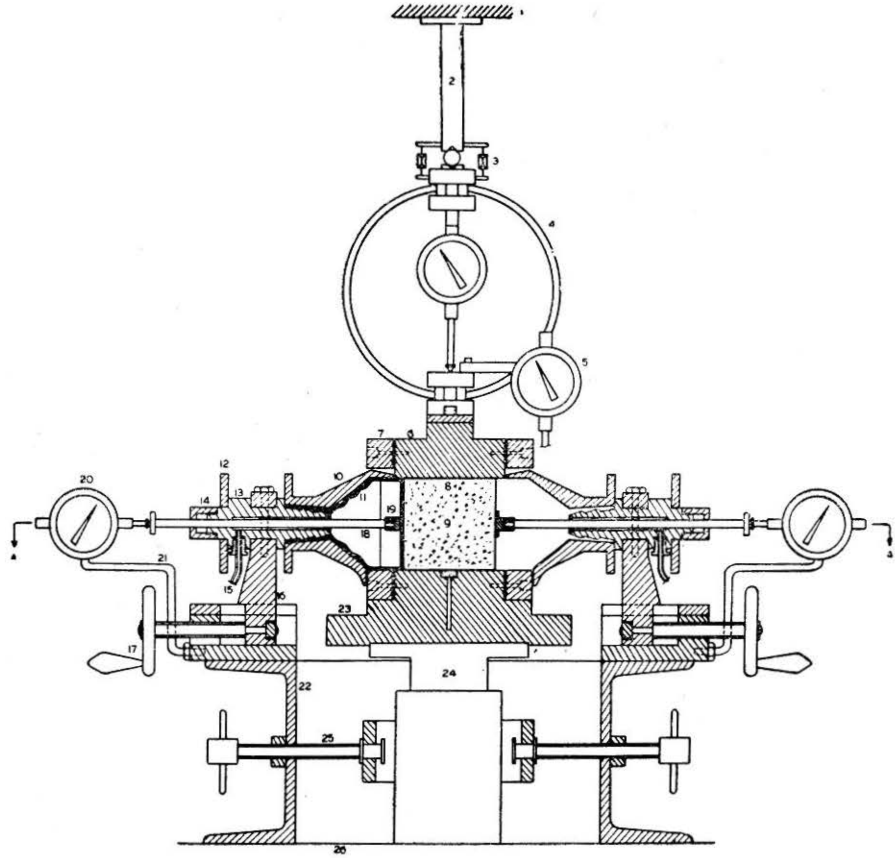

1 Cross beam of loading frame
2 Loading ram
3 Spring
4 Proving ring
5 Dial gauge for axial deformation
6 Loading cap
7 Aluminium segments
8 Sandwhich of lubricated memberanes
9 Soil specimen
10 Rubber bag guide
11 Rubber bag (thickness of rubber sheet exaggerated)
12 Rubber bag and guide clamp
13 Nozzle
14 Cap for nozzle
15 Nylon tube
16 Sliding stand for lateral pressure set up
17 Handle for sliding stand
18 Stainless steel strain rod
19 Stud for connecting strain rod to inside of rubber bag
20 Dial gauge for lateral deformation
21 Stand for dial gauge
22 Raised platform
23 Base of universal triaxial apparatus
24 Ram of loading machine
25 Clamping arrangement
26 Top of loading machine gear box
NB Only one rubber bag is shown—thickness of rubber sheet is shown exaggerated

FIGURE 1*a* Sectional elevation of the universal triaxial apparatus

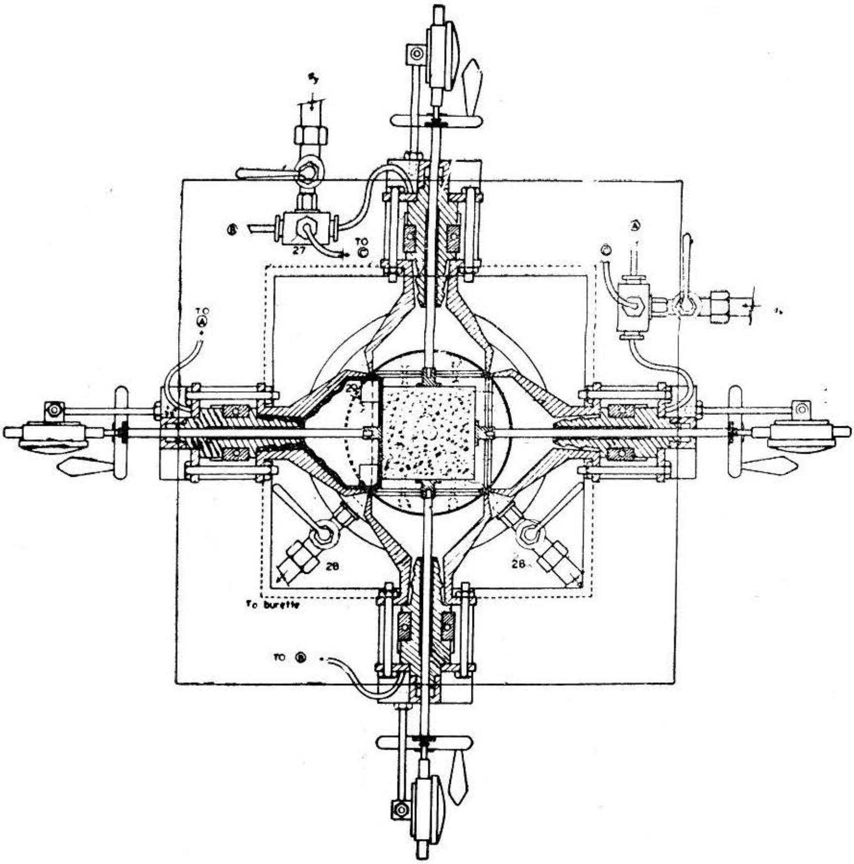

27 T-connection
28 Klinger valve
29 Sponge pieces

NB Only one rubber bag is shown—thickness of rubber sheet is shown exaggerated

FIGURE 1*b* Sectional plan of the universal triaxial apparatus

The modified UTA used for the present investigation differs from the earlier model (Ramamurthy 1970) in the following respects:

(*i*) The design of the guides is changed so as to facilitate extension tests to be conducted at greater axial strain. Side vanes are provided to one pair of the guides to provide support to the sponge pieces embedded in one pair of the rubber bags and also to prevent interference with the adjacent bags. Guides are mounted on movable supports which make the assembling and dismantling of the entire set-us easy.

(*ii*) Aluminium segments used to seal off the specimen are screwed on to the base and top platen to make the specimen enclosed in the rubber membrane completely leak proof.

(*iii*) Shape of the rubber bags is changed to facilitate their preparation with hands, (*iv*) Connection of the rod (which transmits displacement of the vertical faces of the specimen) with the rubber bag is improved and simplified.

(*v*) All the guides are interconnected by a rigid metallic frame to make the system stable and to eliminate any possibility of tilting.

(*vi*) Sample former is screwed on to the base and a collar is provided to keep the membrane in position during preparation of sample and to permit deposition of slightly more quantity of sand above the rim of the body.

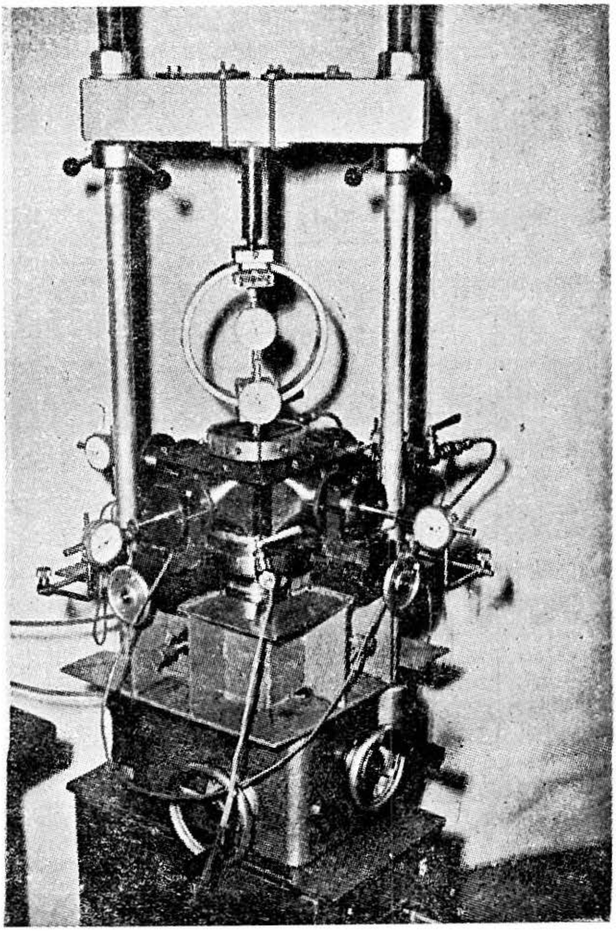

FIGURE 2 General view of the universal triaxial apparatus

Description of Sand and Sample Preparation

Dense, medium dense, and loose specimens of Ottawa sand were tested both in the universal triaxial apparatus and in conventional triaxial apparatus. All tests were carried out on saturated specimens under fully drained condition. Each cubical specimen was prepared using fresh sand sample whereas the sand was reused for preparing cylindrical specimens. The index properties of Ottawa sand are given below.

(*i*) Specific gravity = 2.66; (*ii*) Effective size = 0.43 mm; (*iii*) Coefficient of uniformity = 1.28; (*iv*) 100 per cent passing through B.S. Sieve No. 18 and 100 per cent retained on B.S. Sieve No. 52; (*v*) minimum porosity (by vibrating in a Proctor's mould) = 32.0 per cent; and (*vi*) maximum porosity (Kolbuszewski, 1948) = 41.0 per cent.

For preparing a 7.6 cm cubical specimen, the sand which had been boiled in water and allowed to cool overnight was gently deposited under water with a spoon into the specimen former in three layers. Dense and medium dense specimens were prepared by tamping each layer of the sand with a spatula; the amount of tamping varied depending upon the desired porosity of the sample. When the surface of the sand had reached 6 mm above the rim of the former into the collar, the sides of the former were also tamped lightly with a rubber-tipped mallet. For preparing loose samples, the sand was deposited into the former with a spoon till the surface of the sample had reached 6 mm above the rim of the former into the collar; no tamping was done but the sides of the former were lightly tamped as this was found necessary to spread the sand into the corners of the former.

In each test in the UTA, a sandwich of two 0.35 mm thick rubber membrane was used at the base and the top to minimise end friction acting on the sample; each interface of the sandwich was lubricated with high vacuum silicone grease. No sandwich was placed between the sample sheath and the rubber bags used for applying lateral stresses on the faces of the sample. Faces and sides of the rubber bags were smeared with a thin coating of high vacuum silicone grease to reduce frictional drag on the faces of the sample and for smooth slipping of the bags within the guides.

Figure 3 shows a photograph of the pre-shear sample under suction after removal of the former. A photograph of the post-shear sample is shown in Figure 4. The faces of the specimen, on removal of the guides after the test was over, were plane and there was no evidence of rounding of the corners and bulging of the sample. The sample deformed freely without any interferrence from the parts of the apparatus.

The method of preparation of cylindrical specimens (10.15 cm dia. and 20.30 cm high) of different porosities was similar to that for cubical samples except that the specimens were formed in six layers. No lubricated end platens were used.

Test Programme

The following programme of consolidated drained tests on saturated specimens of Ottawa sand was carried out in the UTA and in the conventional triaxial apparatus:

Tests in the Universal Triaxial Apparatus

All cubical samples tested in the UTA were consolidated by increasing the axial stress and the lateral stresses proportionately in increments up to the desired consolidation pressures. The consolidation pressures in various series of tests and the stresses which were increased or decreased to result

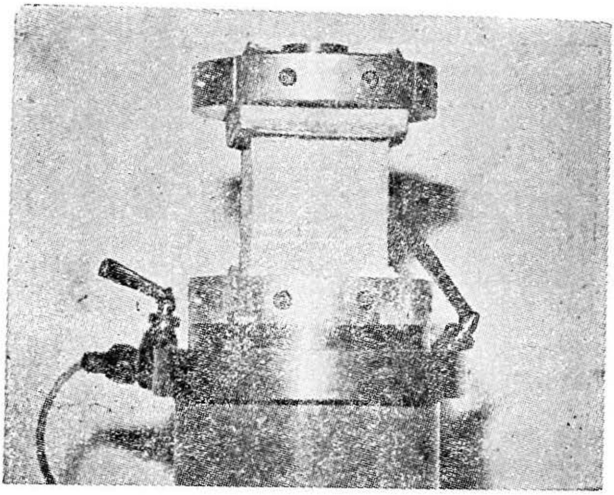

FIGURE 3 Pre-shear sample under suction

failure are shown in Table 1 and described below. It is to be noted that the lateral stresses σ_x' and σ_y' are applied through rubber bags and the vertical stress, σ_z' by raising (for compression tests) or lowering (for extension tests) the platform of the loading machine at a deformation rate of 12 per cent of the specimen height per hour. Reinforced rubber bags (with sponge pieces) were used only in the x-direction when σ_x' was higher than σ_y'. In the description that follows, it may be noted that rubber bags without reinforcement were used both in x- and y-directions only when $\sigma_x' = \sigma_y'$. For comparison, reinforced rubber bags in x-direction were also used when $\sigma_x' = \sigma_y'$.

Series A

Tests were carried out in axisymmetrical condition to compare results obtained from the UTA with those from the conventional triaxial apparatus. In these tests rubber bags without reinforcement were used. The specimens of various porosities were consolidated to the following sets of pressures in x-, y- and z-directions:

(*i*) $\sigma_x' = \sigma_y' = \sigma_z' = 2.05$ kg/cm^2

(*ii*) $\sigma_x' = \sigma_y' = 2.05$ kg/cm^2; $\sigma_z' = 4.10$ kg/cm^2

After consolidation was over, σ_z' was then increased during shear to cause failure of the specimen and, σ_x' and σ_y' were kept constant at 2.05 kg/cm^2.

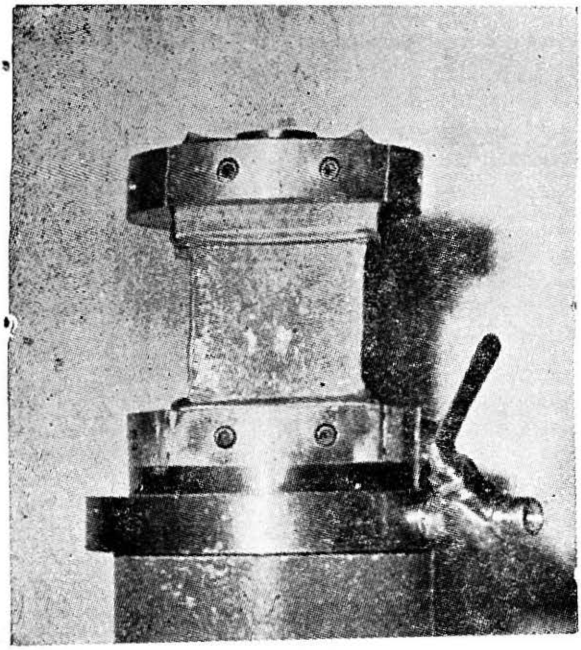

FIGURE 4 Post-shear sample: Series E—plane strain test n_t = 33.8 per cent

Series B

The specimens were consolidated to the following sets of pressures in x-, y-, and z-directions :

	σ'_x	σ'_y	σ'_z	
(*i*)	2.76	2.05	2.05	(kg/cm^2)
(*ii*)	3.47	2.05	2.05	(kg/cm^2)
(*iii*)	4.17	2.05	2.05	(kg/cm^2)

The failure was caused by increasing σ'_z, after consolidation, maintaining σ'_x and σ'_y constant. In this Series reorientation of principal stress directions took place during shearing. During consolidation σ'_x was the major principal stress but at failure σ'_z became the major principal stress thus reorientation of the major principal stress from x- to z-direction occurred during shearing.

TABLE 1 Consolidation Pressures in Various series of Tests in Universal Triaxial Apparatus

Series	Consolidation pressure kg/cm²		
	σ_x'	σ_y'	σ_z'
A	2.05 2.05	2.05 2.05	2.05 ↑ 4.01 ↑
B	2.76 3.47 4.17	2.05 2.05 2.05	2.05 ↑ 2.05 ↑ 2.05 ↑
C	2.76 3.47 4.17	2.05 2.05 2.05	4.10 ↑ 4.10 ↑ 4.10 ↑
D	2.05 ↑	2.05	2.05 ↑
E	2.05 ↑ 2.05 ↑	2.05 2.05	2.05 ↑ 4.10 ↑
F	6.28 6.28 6.28 6.28	6.28 5.57 4.88 4.17	6.28 ↓ 6.28 ↓ 6.28 ↓ 6.28 ↓

Notes: (*i*) Stresses marked with ↑ were increased and those with ↓ were decreased during shear after consolidation.

(*ii*) Rubber bags in *y*-direction were always without sponge reinforcement.

(*iii*) Tests in Series *A* were conducted using rubber bags with and without sponge reinforcement in *x*-direction.

(*iv*) Rubber bags with sponge reinforcement in *x*-direction were always used when $\sigma_x' > \sigma_y'$.

Series C

The specimens were consolidated to the following sets of pressures :

	σ_x'	σ_y'	σ_z'	
(*i*)	2.76	2.05	4.10	(kg/cm²)
(*ii*)	3.47	2.05	4.10	(kg/cm²)
(*iii*)	4.17	2.05	4.10	(kg/cm²)

The failure was caused in a similar manner as in series *B*, i.e., by increasing σ_z' after consolidation and keeping σ_x' and σ_y' constant. Since σ_z' was either equal to or greater than σ_x' when shearing of specimen started, reorientation of principal stress directions did not take place in this series.

Series D

In this series specimens were consolidated isotropically (*i.e.* $\sigma_x' = \sigma_y' = \sigma_z' = 2.05$ kg/cm²) and failure was caused by increasing both σ_x' and σ_z'. The stress σ_x' was increased by raising the self-compensating mercury pot at such a uniform rate that, as far as possible, the desired pressure is attained in *x*-direction at failure and thereafter kept constant during the remaining stage of shearing.

Series E

Specimens were consolidated to the following pressures and then sheared under plane strain condition :

(*i*) $\sigma_x' = \sigma_y' = \sigma_z' = 2.05$ kg/cm²

(*ii*) $\sigma_x' = \sigma_y' = 2.05$ kg/cm²; $\sigma_z' = 4.10$ kg/cm²

During shearing both σ_x' and σ_z' were increased. The stress σ_x' was increased by raising self-compensating mercury pot in such a manner that no deformation was allowed in the *x*-direction (it may be noted that deformation was permitted in *x*-direction during consolidation).

Series F

These were extension tests in which specimens were consolidated to the following pressures :

	σ_x'	σ_y'	σ_z'	
(*i*)	6.28	6.28	6.28	(kg/cm²)
(*ii*)	6.28	5.57	6.28	(kg/cm²)
(*iii*)	6.28	4.88	6.28	(kg/cm²)
(*iv*)	6.28	4.17	6.28	(kg/cm²)

shearing was caused by decreasing σ_z' and maintaining σ_x' and σ_y' constant. At failure σ_z' thus became the minor principal stress and σ_x' the major principal stress.

Tests in the Conventional Triaxial Apparatus

Series H

Compression tests on cylindrical specimens of 10.15 cm dia. and 20.30 cm height were conducted in the conventional triaxial apparatus. The initial porosity of the specimens ranged from 34.0 to 39.5 per cent. The specimens of Ottawa sand were isotropically consolidated to three different cell pressures 1.0, 2.0 and 3.0 kg/cm². All the cylindrical specimens were sheared at a deformation rate of 12 per cent per hour.

Discussion of Test Results

Comparison of Axisymmetric Compression Test Results from CTA and UTA

In order to judge the performance of the universal triaxial apparatus (UTA), the test results under axisymmetric conditions will be compared with those obtained from the conventional triaxial apparatus (CTA) which has been in use as a standard apparatus for simplicity of its operation. The limitations of the conventional triaxial apparatus are well known. Bishop and Green (1965) demonstrated that the peak strength and volumetric strain rate at failure for short sample (height to diameter ratio 1 : 1) with adequately lubricated platens was the same as that of a conventional 2 : 1 sample with rough platens at each end of the specimen. They also observed that both the axial strain and dilation of 1 : 1 sample adequately lubricated were greater in magnitude than those for conventional 2 : 1 sample at the same porosity and that the stress-strain curves for the two types of samples were not the same.

Stress-Strain Characteristics—The stress-strain and volumetric strain curves for typical dense and medium dense sample of Ottawa sand tested in the CTA and in the UTA are shown in Figures 5 and 6. The early part of the stress-strain curve of the cylindrical sample is slightly steeper than that of the cubical sample of almost similar initial porosity. The cylindrical sample fails at a lower axial strain compared to cubical sample. Nevertheless, the observed strengths of both samples are almost identical. The greater steepness of the axial stress-strain curve and the lower axial strain of the cylindrical samples compared to cubical samples could be accounted for non-uniform stress and strains near each end of the cylindrical sample caused by the end restraint due to rough platens.

Peak Strengths—The variation of peak strength of cylindical and cubical samples of Ottawa sand over a complete range of initial porosities is shown in Figure 7. There appears to be little difference in the strength-porosity relationships of cylindrical and cubical samples. The mean curve of cubical samples gradually diverges from the mean curve of cylindrical samples and shows an increase of approximately 1° for the loose samples when the results are compared independently. Considering the scatter generally observed with the loose samples it could be concluded that the strength-porosity relationship of the cubical samples (with adequate lubrication) tested in the UTA under axisymmetric conditions is almost identical with that of the cylindrical samples (with rough porous stones at each end) tested in the CTA.

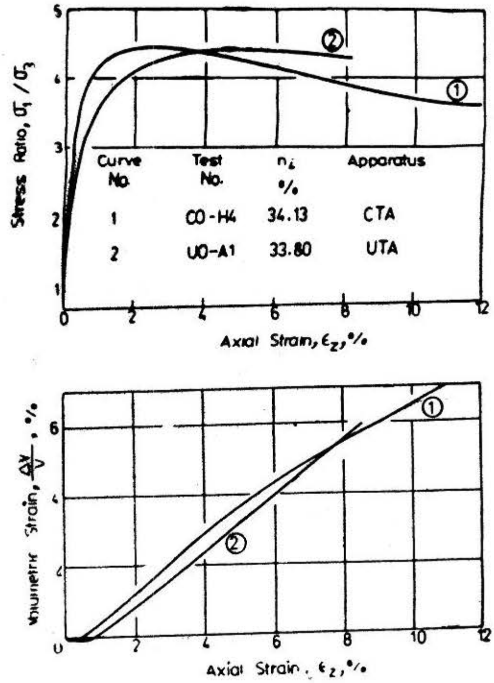

FIGURE 5 Comparison of stress-strain volume change characteristics of dense samples of Ottawa sand under axisymmetric compression in CTA and UTA

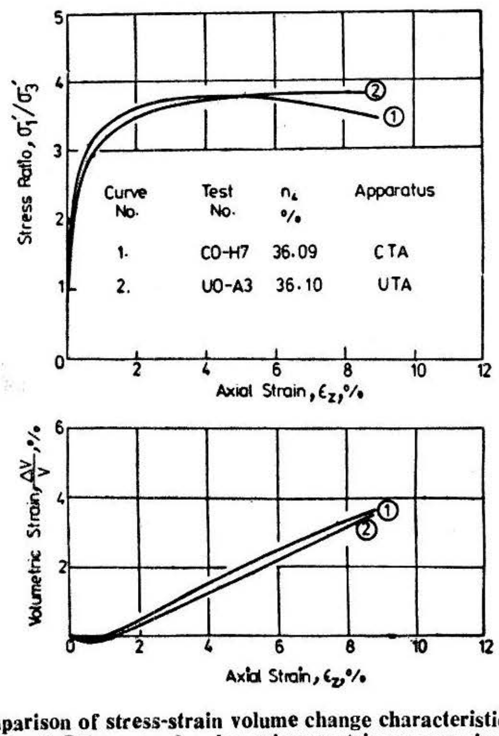

FIGURE 6 Comparison of stress-strain volume change characteristics of medium dense sample of Ottawa sand under axisymmetric compression in CTA and UTA

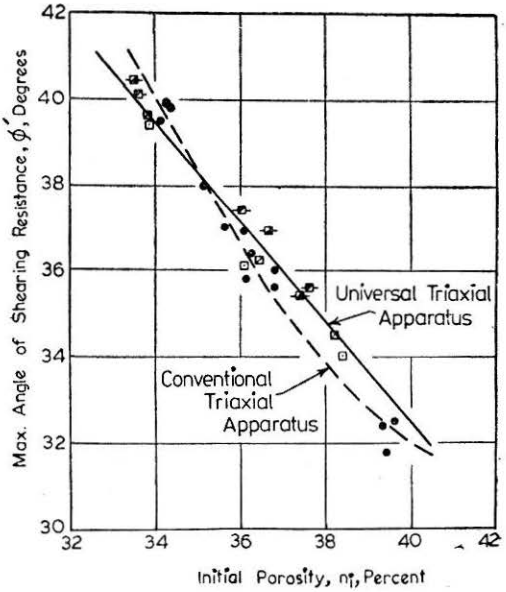

FIGURE 7 Comparison of peak strength of Ottawa sand in CTA and UTA in axisymmetrical compression

Axial Strains at Failure—It may be seen from Figure 8 that the axial strains at failure for cylindrical and cubical samples of Ottawa sand are not similar. The axial strain to failure for the dense cubical sample adequately lubricated is approximately twice that obtained for a 2:1 cylindrical sample with rough platens and is about 1.5 time for the loose samples. As pointed out earlier that the lower axial strain at failure of the cylindrical sample compared to cubical sample might be due to the end restraint in the cylindrical sample causing non-uniform stresses and strains. End restraint seems to introduce certain degree of brittle nature of failure in the specimen.

Volumetric Strain Rates at Failure—The volumetric strain rates (defined as the slope of the volumetric strain-axial strain curve) at failure for both cylindrical and cubical samples of Ottawa sand plotted against the initial porosities are shown in Figure 9. The points corresponding to the cylindrical samples lie closer to the mean curve of the cubical samples. This indicates that the rate of dilation (with respect to the major principal strain) is almost similar for both cylindrical samples (in CTA) and cubical samples (in UTA).

The relationships between the maximum angle of shearing resistance and the volumetric strain rate at failure for cylindrical and cubical samples are shown in Figure 10. In each case a straight line is obtained with very little scatter but the mean curve for the cylindrical samples gradually diverges from the mean curve for the cubical samples as the initial porosity increases. This is due to the fact that slightly higher value of peak strength is obtained for the loose cubical sample (in UTA) than that for the cylindrical sample (in CTA) of the same initial porosity.

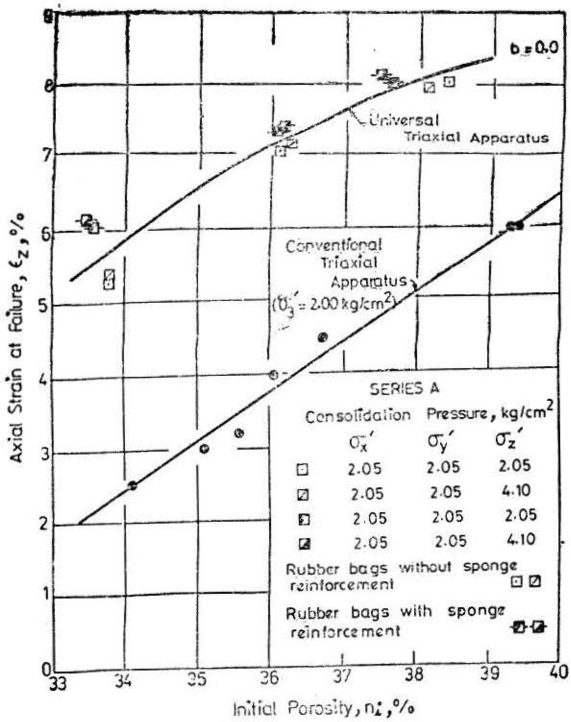

FIGURE 8 Comparison of axial strains at failure of samples of Ottawa sand under axisymmetric compression in CTA and UTA

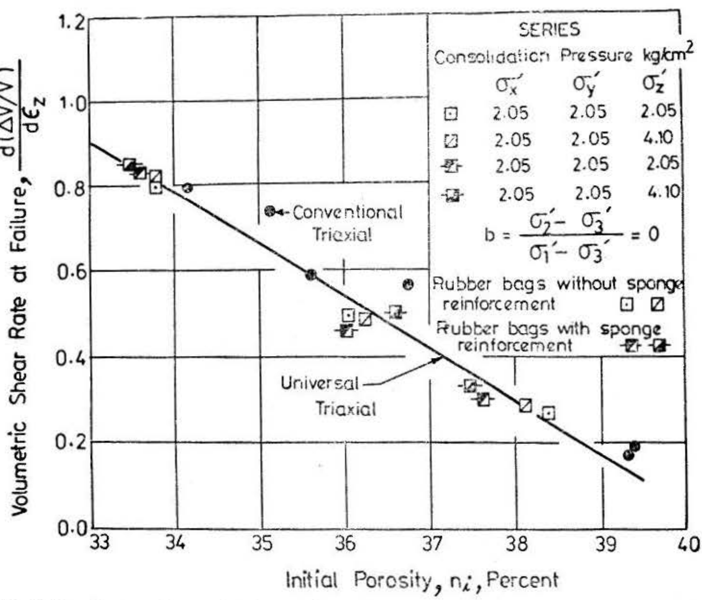

FIGURE 9 Comparison of volumetric strain rate at failure of samples of Ottawa sand under axisymmetric compression in CTA and UTA

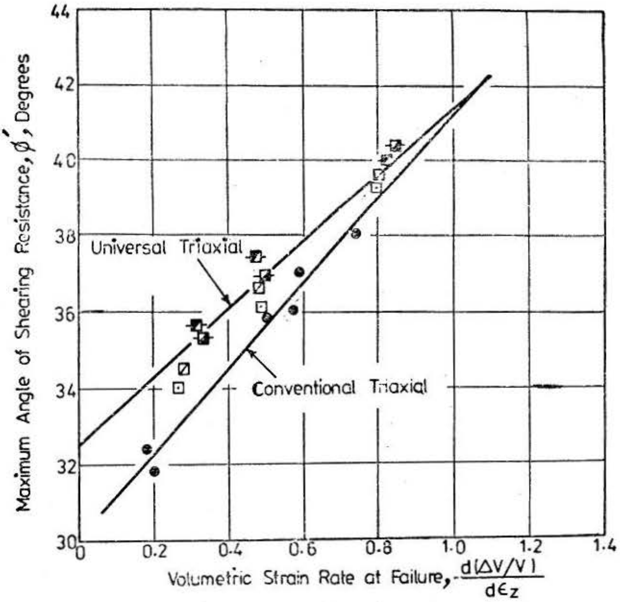

FIGURE 10 **Relationship between maximum angle of shearing resistance and volumetric strain rate at failure of samples of Ottawa sand under axisymmetric compression in CTA and UTA**

It has thus been demonstrated that in the case of compression tests under axisymmetric conditions, practically identical results in terms of the peak strength and the volumetric strain rate at failure are obtained from the conventional triaxial apparatus and the universal triaxial apparatus over a complete range of porosities. The steeper stress-strain curves and the lower axial strain at failure of the conventional 2:1 cylindrical sample with rough platens compared to adequately lubricated cubical sample in the UTA are attributed to the difference in end conditions.

Tests in the UTA Under General Stress System with Different Stress Paths

In this section the results of drained compression, plane strain and extension tests conducted on cubical samples of Ottawa sand with different stress paths are presented for the complete porosity range varying from dense (n_i=33.5 per cent) to loose (n_i=38.0 per cent). Detailed discussion on the results of plane strain tests will be presented in a separate paper. The consolidation pressures in various series of tests and the stresses which were increased or decreased to produce failure have already been discussed earlier.

Stress-Strain Characteristics—The stress-strain curves obtained from compression tests (Series B, C and D) and Extension tests (Series F) on dense samples of Ottawa sand are shown in Figures 11 through 14 with a view to examine influence of the intermediate principal stress in each series of tests individually. Temporarily disregarding the small difference in the initial porosities of the samples, it may be seen that in

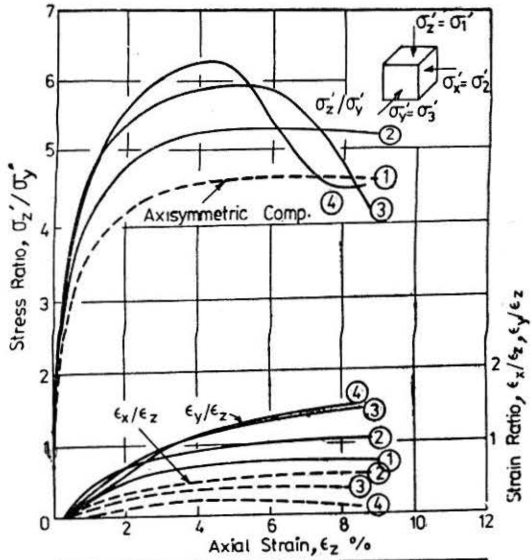

Curve No.	Test No.	n_i %	Consolidation Pressures, kg/cm^2 σ_x'	σ_y'	σ_z'
①	UO-A9	33.6	2.05	2.05	2.05
②	UO-B1	33.6	2.76	2.05	2.05
③	UO-B2	33.9	3.47	2.05	2.05
④	UO-B3	33.9	4.17	2.05	2.05

FIGURE 11 Influence of intermediate principal stress on stress-strain characteristics of dense samples of Ottawa sand in Series B

the compression tests (Series B, C and D) the initial slope of the stress-strain curve increases with increasing value of the intermediate principal stress and the curve drops off more rapidly after the peak. The peak strength increases and the axial strain, ϵ_z, at failure decreases with increasing intermediate principal stress. The ratio of the intermediate principal strain, ϵ_x, the major principal strain, ϵ_z, continually decreases wheraas the ratio of the minor principal strain, ϵ_y, to the major principal strain, ϵ_z, continually increases with increasing value of the intermediate principal stress. Similar behaviour is also seen from compression tests on medium dense and loose samples of Ottawa sands.

In the extension tests (Series F), the initial slope of the stress-strain curve (Figure 14) increases with decreasing value of the intermediate principal stress [$b = (\sigma_2' - \sigma_3') / (\sigma_1' - \sigma_3')$ decreases frombeing equal to 1.0 to approximately equal to 0.6]. This is in contrast to that seen in compression tests (Series B, C and D) in which the initial slope of the stress-strain curve increases as the value of b increases. This difference in behaviour of stress-strain curves is due to the stress path followed in extension (mean normal stress decreasing) and compression tests (mean normal stress increasing), But their is similarity when considered from the point of view of changing stress conditions from axisymmetric to more

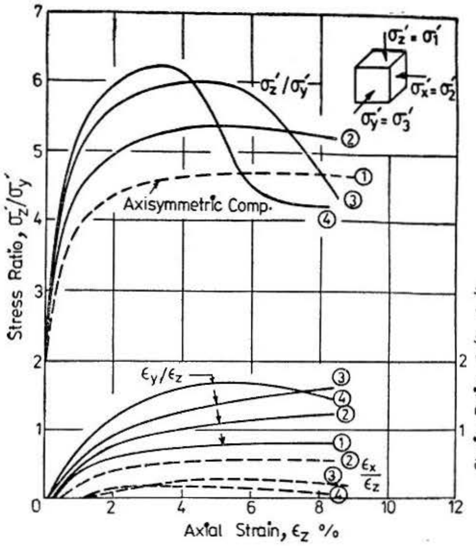

Curve No.	Test No.	n_i %	Consolidation Pressures, kg/cm² σ_x'	σ_y'	σ_z'
①	UO-A10	33.5	2.05	2.05	4.10
②	UO-C1	33.5	2.76	2.05	4.10
③	UO-C2	33.3	3.47	2.05	4.10
④	UO-C3	33.3	4.17	2.05	4.10

FIGURE 12 **Influence of intermediate principal stress on stress-strain characteristics of dense samples of Ottawa sand in series C**

unsymmetric one. Similar behaviour is also seen in extension tests on medium dense and loose samples of Ottawa sand. For a given density, the axial strain to failure decreases as the stress conditions change from axisymmetric ($b = 1.0$) to more unsymmetric ($b \approx 0.6$) similar to that observed in compression tests in the region $b = 0$ to $b = 0.3$.

In Figures 15 and 16 are shown the stress-strain curves from tests on respectively dense and loose samples of Ottawa sand having attained almost the same peak strength in Series B, C and D. There is slight difference in the initial porosities of samples selected for compression and the values of b at failure are also different. It may be seen from these curves that despite having almost the same peak strength the stress-strain (axial) curves and the resulting lateral strains are influenced by the stress path followed in series B, C and D. The early part of the stress-strain curve from series C ($\sigma_z' / \sigma_y' = 2$ during consolidation) is steeper than that obtained from series B and D in which the ratio σ_z' / σ_y' was equal to one during cosolidation. The sample in Series C dilates more compared to the samples in Series B and D.

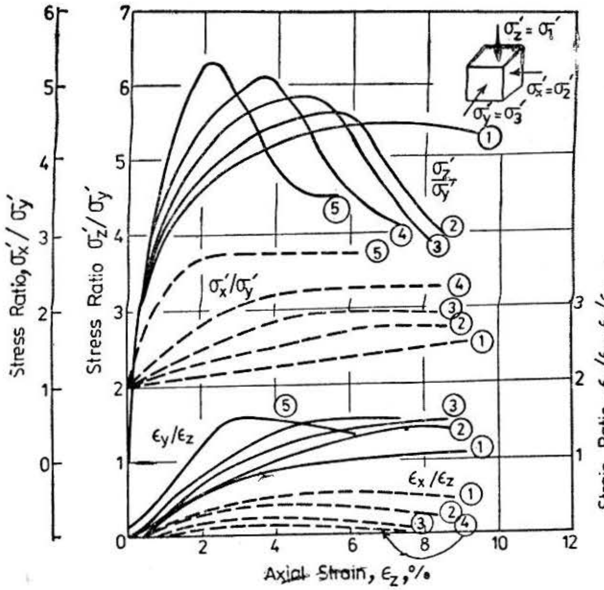

Curve No.	Test No.	n_i %	Pressure at failure kg/cm² σ_x'	σ_y'	σ_z'
1	UO-D1	33.4	2.87	2.05	11.18
2	UO-D2	33.5	3.40	2.05	11.39
3	UO-D3	33.5	3.89	2.05	11.95
4	UO-D4	33.7	4.55	2.05	12.40
5	UO-D5	33.8	5.61	2.05	12.81

FIGURE 13 **Influence of intermediate principal stress on stress-strain characteristics of dense samples of Ottawa sand in Series D (all samples were isotropically consolidated to an all-round pressure of 2.05 kg/cm²)**

Peak Strengths

The peak strengths from tests in Series A, B, C, D, E and F have been adjusted to correspond to initial porosities of 33.5 per cent (dense), 36.5 per cent (medium dense) and 38.0 per cent (loose) by interpolating between the slopes of peak strength-initial porosity curves (not presented here). These interpolated peak strengths have been plotted against *b* in Figure 17 for dense, medium dense, and loose samples. An approximately linear increase in peak strength is obtained for samples of a given porosity until a value of *b* approximately equal to 0.30 is reached. The influence of stress path on peak strength of dense samples for values of *b* at failure beyond 0.1 is clearly indicated in Figure 17; for the same value of *b*, the peak strength from series D is lower than that obtained from Series B and C. In the case of medium dense and loose samples, the peak strengths are found to be relatively unaffected by the stress path followed. Other investigators (mentioned in the next paragraph) have also suggested that

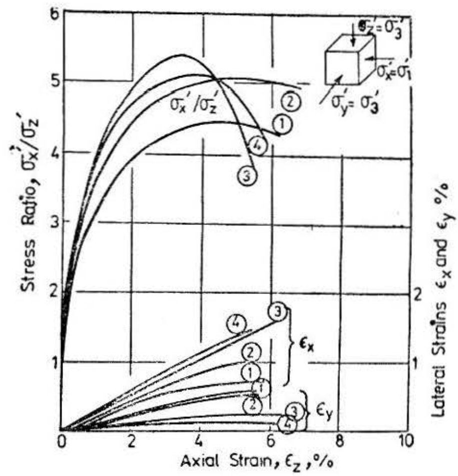

Curve No.	Test No.	n_i %	Consolidation Pressures, kg/cm^2 σ_x'	σ_y'	σ_z'
1	UO-F1	33.6	6.28	6.28	6.28
2	UO-F2	33.7	6.28	5.57	6.28
3	UO-F3	33.6	6.28	4.88	6.28
4	UO-F4	33.7	6.28	4.17	6.28

FIGURE 14 Influence of intermediate principal stress on the stress-strain characteristics of dense samples of Ottawa sand in extension tests (series F)

for drained tests on sands with monotonically increasing shear stresses under the relatively limited conditions so far investigated, the peak strength may be independent of the stress path followed. The value of b at failure in plane strain tests is found to increase with increasing porosity.

The increase in peak strengths of sands when the intermediate principal stress increases from being equal to the minor principal stress to the value required to maintain conditions of zero lateral yield (plane strain) has *also been observed by other investigators using different types of apparatus*; see Bell (1965), Bemben (1967), Esrig and Bemben (1965), Ko (1966), Ko and Scott (1968), Lomize and Kryzhanovsky (1967), Lomize, Kryzhanovsky and Vorontsov (1969), Malyshev and Fralis (1968), Green (1969 and 1971*a*), Green and Bishop (1969), Mesdary (1969), Sutherland and Mesdary (1969), Dyson (1970), Reades (1972), Lade and Duncan (1973), and Ramamurthy and Rawat (1973).

It may be seen from Figure 17 that as the value of b increases from 0.3 the peak strength continually decreases and at $b = 1$ $\left(i.e., \sigma_1' = \sigma_2'\right)$ the extension peak strength is almost identical to that obtained at $b = 0$ $\left(i.e.\ \sigma_2' = \sigma_3'\right)$ in compression tests. There appears to be significant divergence in the results obtained by various investigators using different type of apparatus in the region b equal to that corresponding to plane

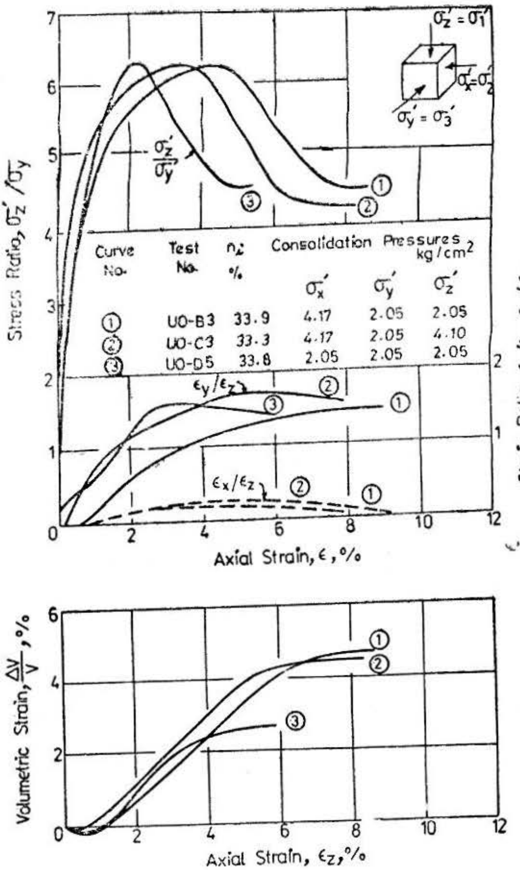

FIGURE 15 Influence of stress path on stress-strain-volume change characteristics of dense samples of Ottawa sand

strain condion to $b = 1.0$. Some researehers have found that the strength near $b = 1$ is approximately equal to or greater than that in a plane strain test (Ko, 1966; Ko and Scott, 1967, 1968; Lomize & Kryzhanovsky, 1967, Green, 1969, 1971*a*; Green and Bishop, 1969, Bishop 1967*a*; Reades, 1972; Lade and Duncan, 1973) while others have obtained a reduction in strength as $b \to 1$ (Malyshev and Fralis, 1968; Mesdary, 1969; Sutherland and Mesdary, 1969; Mesdary and Sutherland, 1970; and Sutherland, 1971).

Reades (1972) observed the marked difference in peak strength due to variation in the method of loading in the region $0.6 < b < 1.0$. His results of tests on loose samples are reproduced here (Figure 18). It may be seen that the peak strengths from the tests with both pairs of rigid platens closing (mean normal stress increasing) increase as the value of b increases from $b \approx 0.6$ whereas the peak strength decreases from the tests in which the axial stress is reduced (mean normal stress decreasing) to failure. The latter stress path in which the major principal stress was reoriented to a horizontal direction was similar to that used by Mesdary (1969) and also used in the present investigation. Thus, it can be concluded that under

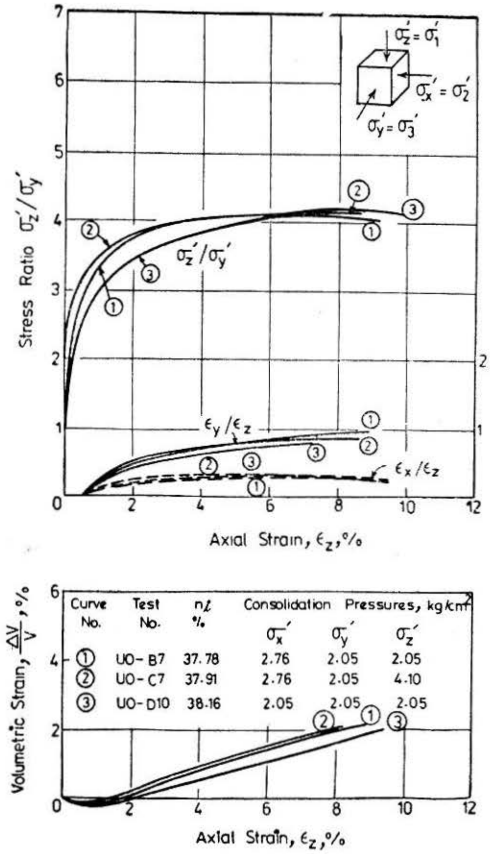

FIGURE 16 **Influence of stress path on stress-strain-volume change characteristics of loose samples of Ottawa sand**

similar stress path (mean normal stress decreasing), the peak strengths decrease as the value of b increases from 0.6 to 1.0. The results of present investigation conform to this peak strength—b relationship in the region $b = 0.6$ to $b = 1.0$.

Linear Strains at Failure

The interpolated values of axial strains, ϵ_z, at failure corresponding to initial porosities of 33.5 per cent (dense), 36.5 per cent (medium dense) and 38.0 percent (loose) are plotted against b and shown in Figure 19 the value of ϵ_z at failure decreases with the increasing value of b at failure in the region $0 < b < 0.30$. There is a marked difference in the values of ϵ_z at failure in Series D in which both σ_z' and σ_x' were increased during shearing and those from Series B and C in which only σ_z' was increased to failure. This clearly demonstrates the influence of the stress path of the axial strains ϵ_z at failure. When the mean curve from Series D is extrapolated to intersect at

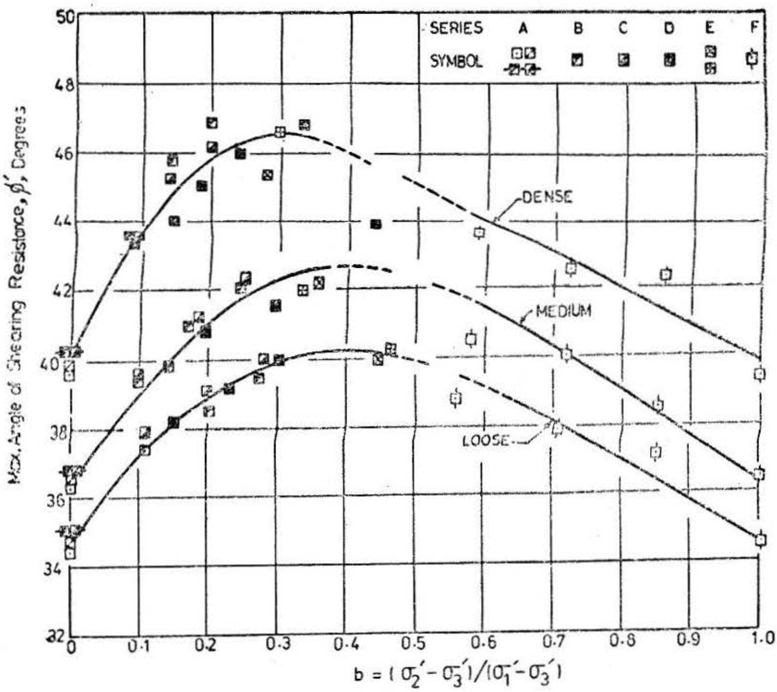

FIGURE 17 Comparison of maximum angle of shearing resistance at failure for dense ($n_i = 33.5\%$), medium dense ($n_i = 36.5\%$), and loose ($n_i = 38.0\%$) samples of Ottawa sand

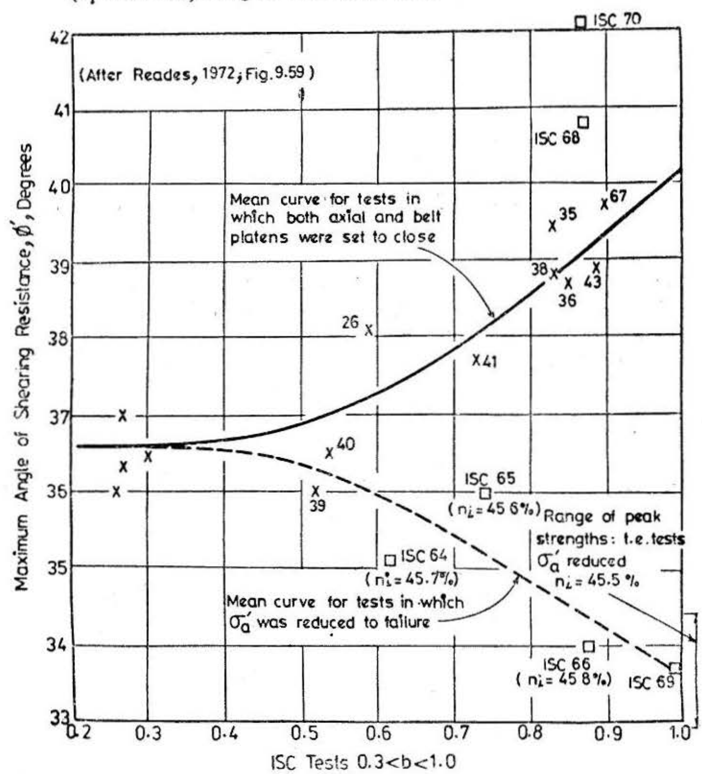

FIGURE 18 Comparison of peak strength for loose samples ($n_i = 45.5\%$) for tests in which the stress path to failure was varied with previous ISC tests and more conventional triaxial extension tests

$b=0$ axis, the value of ϵ_z is found to be about 1.4 times of the value for tests under axisymmetric conditions. Green (1969, 1971*a*) found that the extrapolated value of the axial strain for a dense sample in the independent stress control (ISC) apparatus was twice the value measured in a test at $b=0$. On the other hand, Reades (1972) using the same ISC apparatus found close agreement between dense samples (after applying correction for axial platen ratio) as $b \rightarrow 0$ and compression tests at $b=0$. Reades pointed out that the discontinuity in the axial strain at failure curve might perhaps be due to a change in sample behaviour between $b = 0$ and $b = 0.15$. For extension tests in the region $b \simeq 0.6$ to $b = 1.0$, it may be seen that for a given porosity, the axial strain ϵ_z (expansive) at failure increases with increasing value of b i.e. it is more for axisymmetrical extension test than in unsymmetrical case. For the same value of b at failure, as the initial porosity of the sample increases, ϵ_z at failure also increases.

The interpolated values of lateral strain, ϵ_x, at failure in x-direction are plotted against b and shown in Figure 20. At failure ϵ_x decreases with increasing value of b at failure and this curve meets the points corresponding to plane strain tests (Series E) in which no deformation in x-direction was permitted (*i.e.* $\epsilon_x=0$). For the same value of b at failure, the value of ϵ_x at failure in Series D is slightly more than those from Series B and C for medium dense and loose samples. For extension tests in the region $b \simeq 0.6$ to $b=1.0$, the linear strains ϵ_x (compressive) at failure are found to decrease slightly with increasing b.

The plots (Figure 21) of the lateral strains, ϵ_y, at failure in y-direction versus b indicate that in Series B and C, the lateral strain ϵ_y at failure first increases with increasing value of b up to about 0.1 and then decreases with further increase in the value of b. The influence of the stress path is clearly indicated by the greater values of ϵ_y at failure in Series D compared to those from Series B and C at the same value of b at failure. The extrapolated values of ϵ_y at failure are also greater than those for axisymmetric compression tests at $b=0$. Comparison of linear strains ϵ_y (compressive) at failure in extention tests (Series F) indicates that as b increases from $b \simeq 0.6$ to $b=1.0$, ϵ_y also increases. For the same value of b at failure, ϵ_y increases only slightly with increasing initial porosity.

Volumetric Strains and Volumetric Strain Rates at Failure

Figure 22 indicates that for dense and medium dense samples the volumetric strains decrease with increasing value of b at failure in compression tests whereas in the case of loose samples the volumetric strains remain essentially constant upto $b=0.1$ and then decreases as the value of b at failure increases further up to 0.3. The extrapolated values of volumetric strains at failure in Series D are again greater than the corresponding values in axisymmetric compression tests at $b=0$. In extension tests (Series F), the volumetric strains at failure increase with increasing value of b for dense samples but remains almost constant for medium dense and loose samples.

For medium dense and loose samples the volumetric strain rates at failure (with respect to axial strain ϵ_z) are essentially constant in the region $0 < b < 0 3$ (Figure 23) while the peak strength increases. But in the

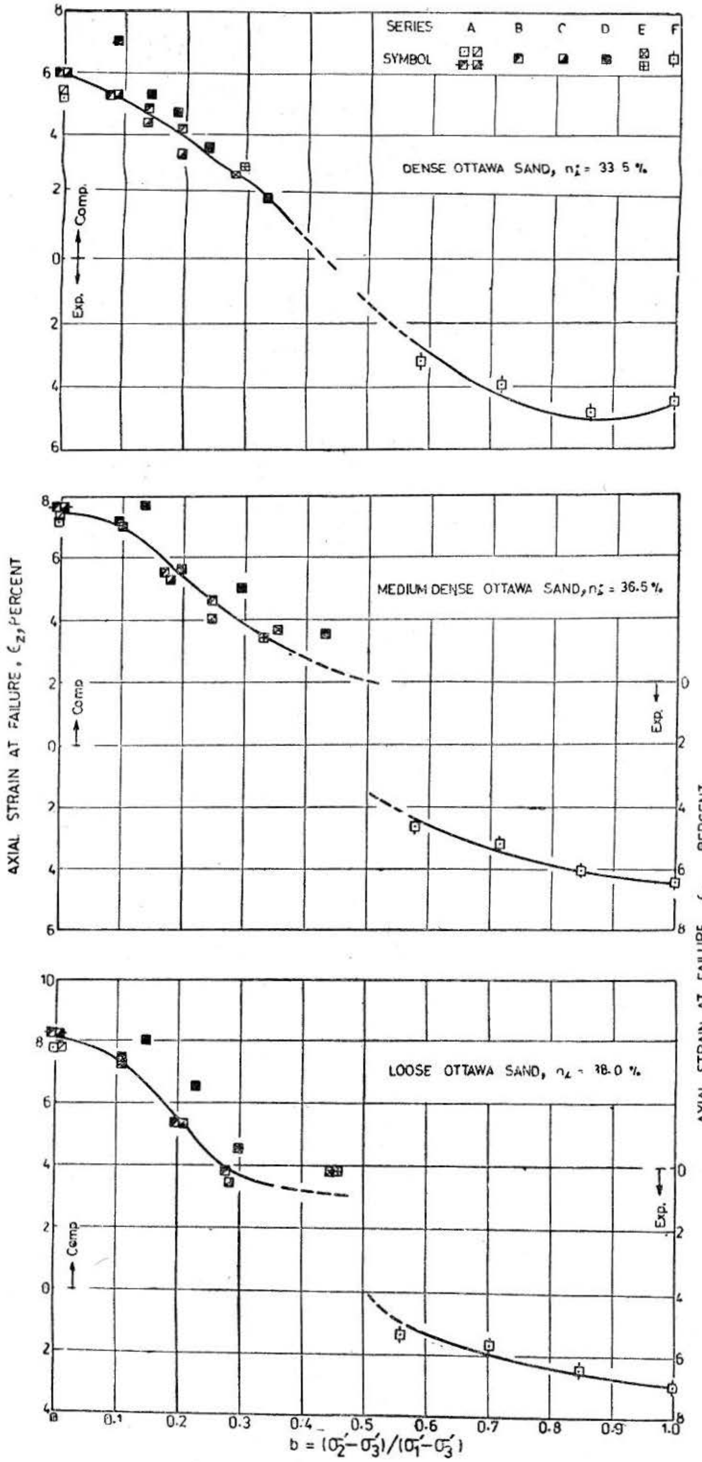

FIGURE 19 Comparison of axial strain in z-direction at failure for dense ($n_i = 33.5\%$), medium dense ($n_i = 36.5\%$), and loose ($n_i = 38.0\%$) samples of Ottawa sand

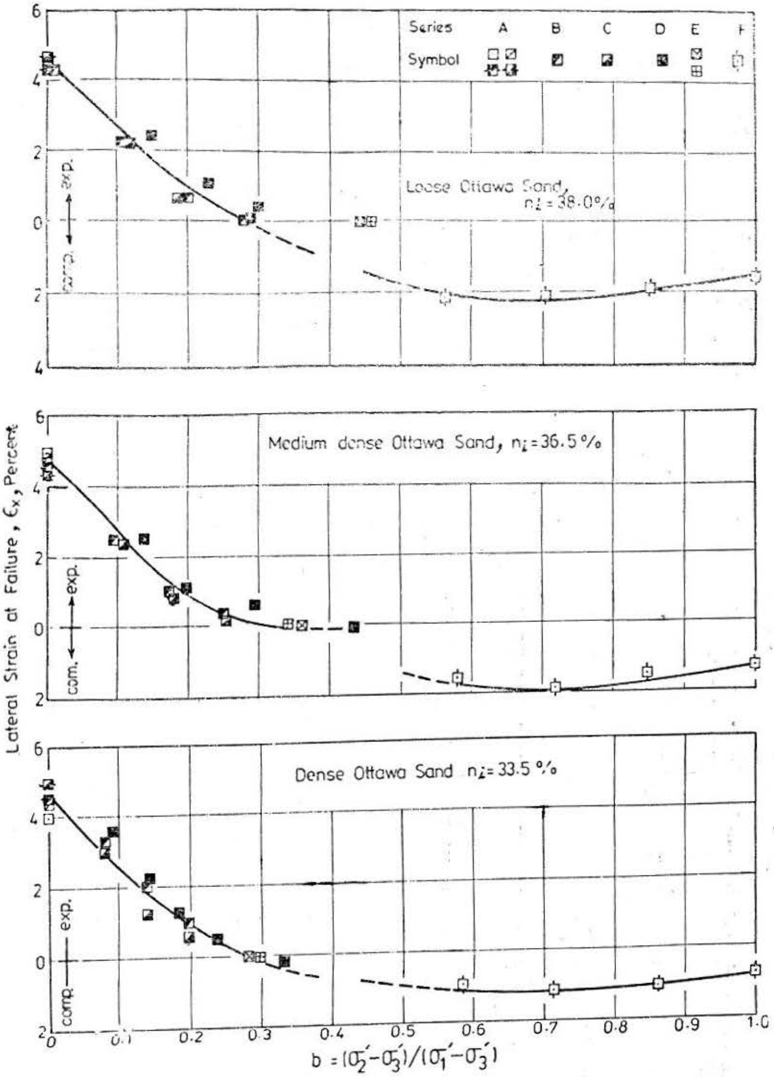

FIGURE 20 **Comparison of lateral strain in x-direction at failure for dense ($n_i=33.0\%$) medium dense ($n_i=36.5\%$) and loose ($n_i=38.0\%$) samples of Ottawa sand**

case of dense samples the volumetric strain rates increase almost linearly from $b=0$ to $b=0.3$. This is in contrast with Green's hypothesis (based on his results on dense samples in the ISC apparatus) that there would be virtually no change in the dilatancy rate in the region $0 < b < 0.3$. However, the results of tests on medium dense and loose samples in UTA substantiate Green's hypothesis in the region $0 < b < 0.3$. There appears to be no influence of the intermediate principal stress on the volumetric strain rates in the region $b \simeq 0.6$ to $b=1.0$; the volumetric strain rates are constant while the peak strength decreases.

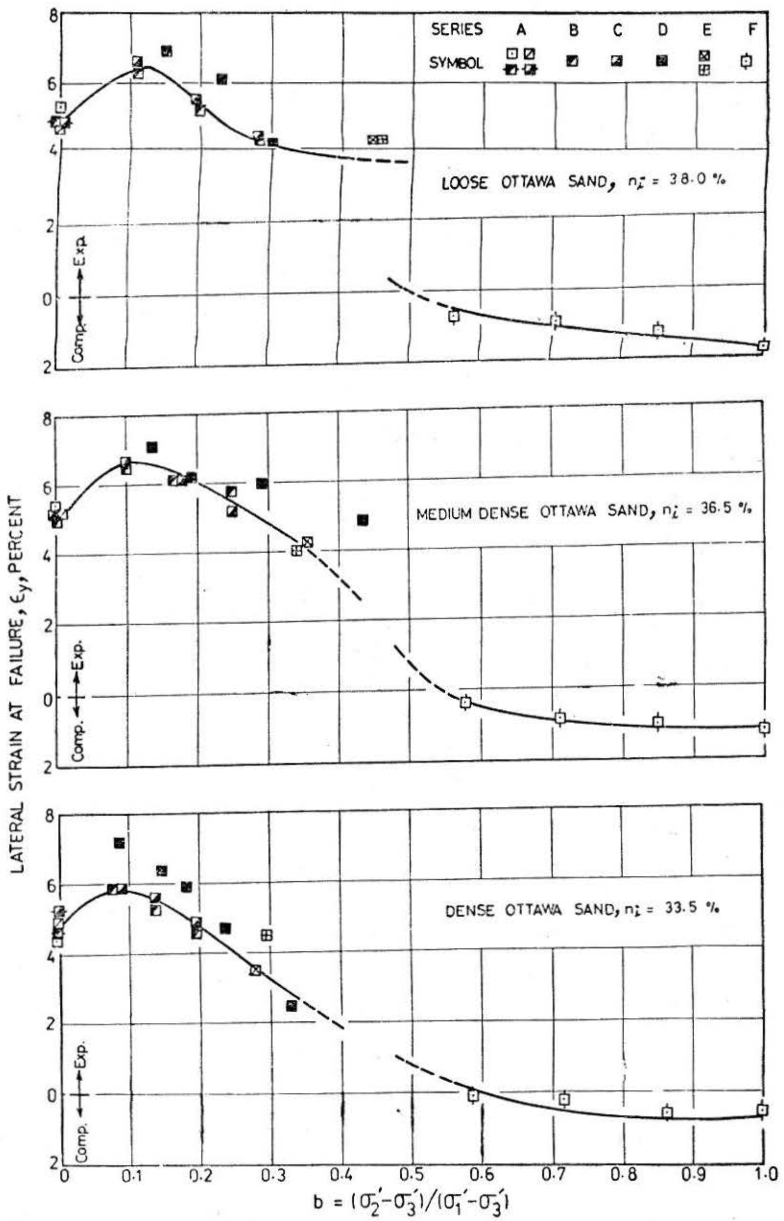

FIGURE 21 **Comparison of lateral strain in *y*-direction at failure for dense (n_i=33.5%), medium dense (n_i=36.0%), and loose (n_i=38.0%) samples of Ottawa sand**

Ratio of Octahedral Shear Stress and Octahedral Normal Stress

In the compression tests, the ratio of octahedral shear stress (τ_{oct}) to the octahedral normal stress (σ_{oct}) at failure is found to decrease with increasing initial porosity and with increasing intermediate principal stress. A

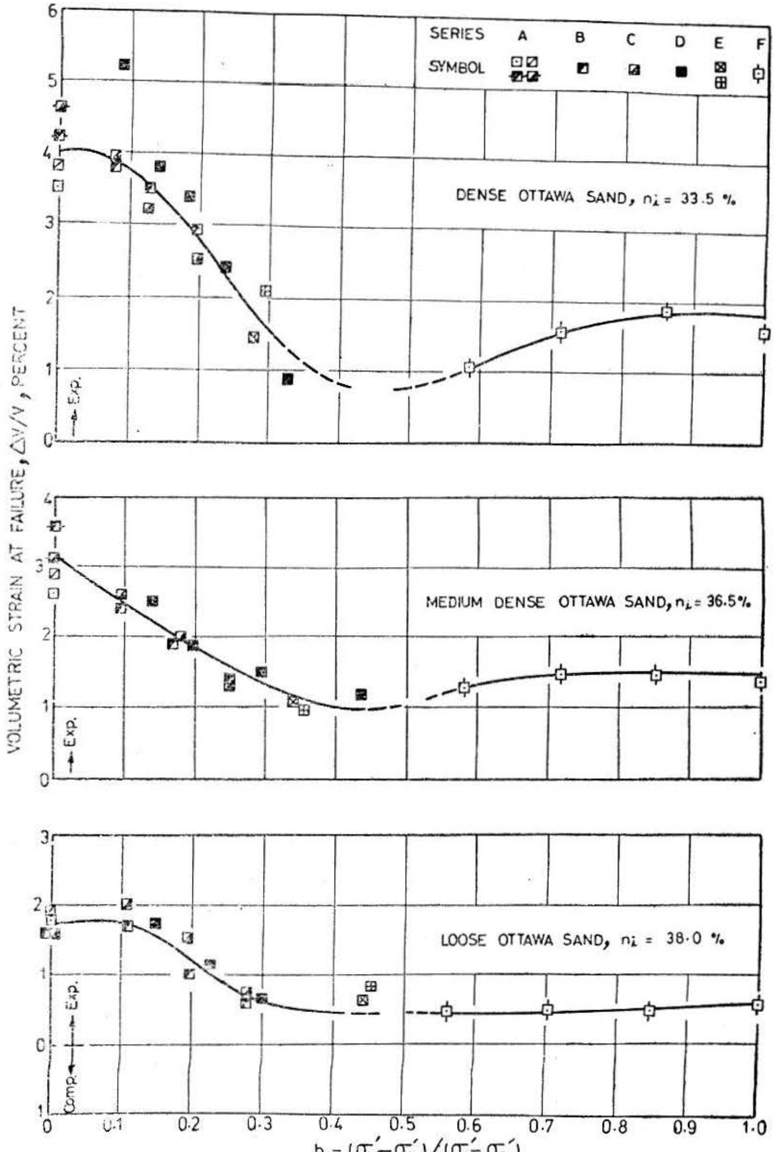

FIGURE 22 Comparison of volumetric strain at failure for dense (n_i=33.5%), medium dense (n_i=36.0%), and loose (ni=38.0%) samples of Ottawa sand

typical set of curves for Series B is shown in Figure 24. This ratio interpolated to correspond to initial porosities of 33.5 per cent, 36.5 per cent and 38.0 per cent is ploltted against the octahedral shearing strains at failure in Figure 25. It may be seen that for a given porosity, a unique relationship is obtained between the ratio (τ_{oct}/σ_{oct}) at failure and the octahedral shearing strain (r_{oct}) at failure.

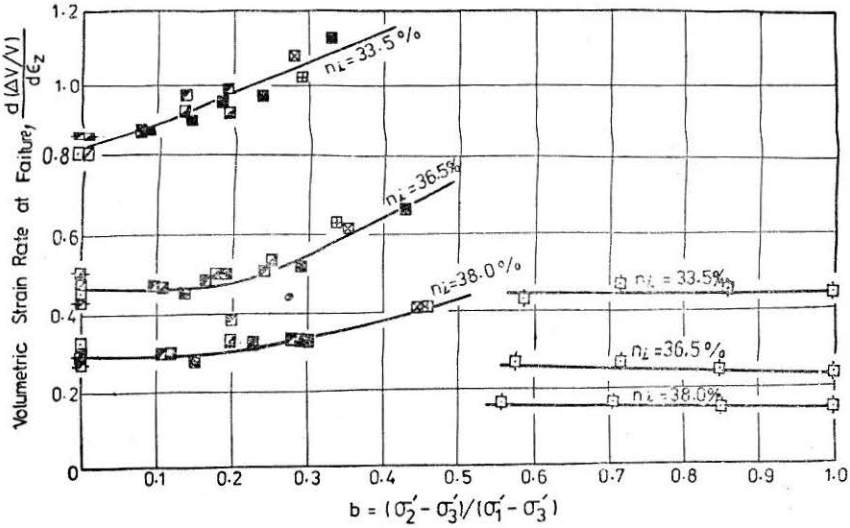

FIGURE 23 Comparison of volumetric strain rate at failure (Series A to F)

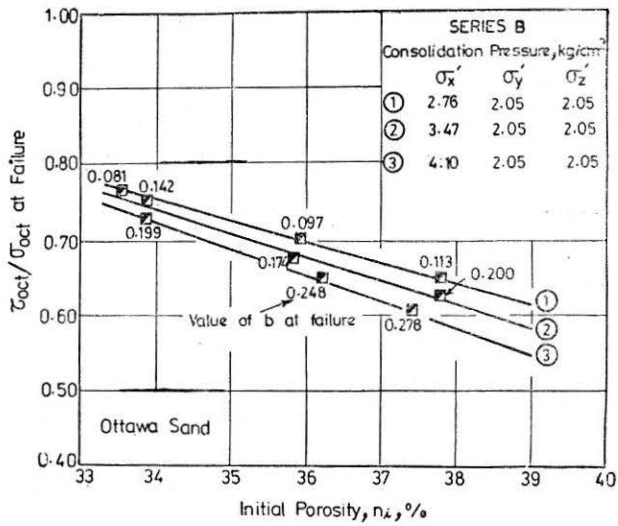

FIGURE 24 Variation of ratio of octahedral shear and octahedral normal stress at failure with initial porosity in Series B

In the extension tests (Series F), the ratio (τ_{oct}/σ_{oct}) at failure is found to decrease with increasing porosity and with increasing intermediate principal stress (Figure 26) as found in compression tests. This ratio extrapolated to correspond to initial porosities of 33.5 per cent, 36.5 per cent and 38.0 per cent is plotted against corresponding octahedral shearing strains r_{oct} in Figure 27. It may be seen that irrespective of initial porosities of samples, the ratio (τ_{oct}/σ_{oct}) is uniquely related to octahedral shearing strains r_{oct} at failure. This relationship differs in two respects from that obtained from

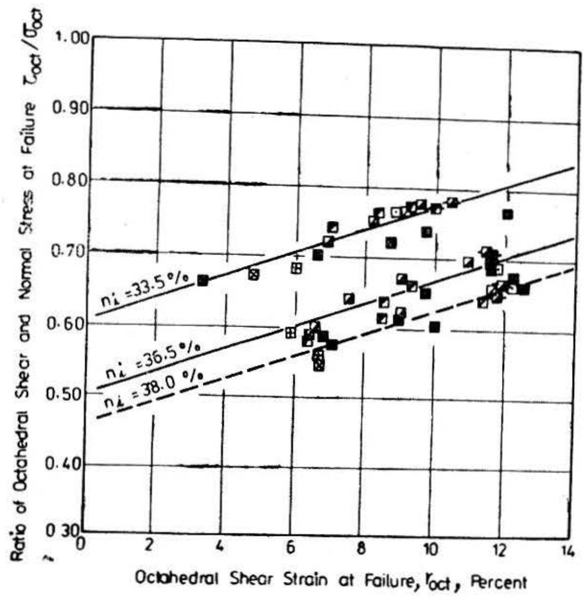

FIGURE 25 Relationship between ratio of octahedral shear and octahedral normal stress at failure and octahedral shear strain at failure

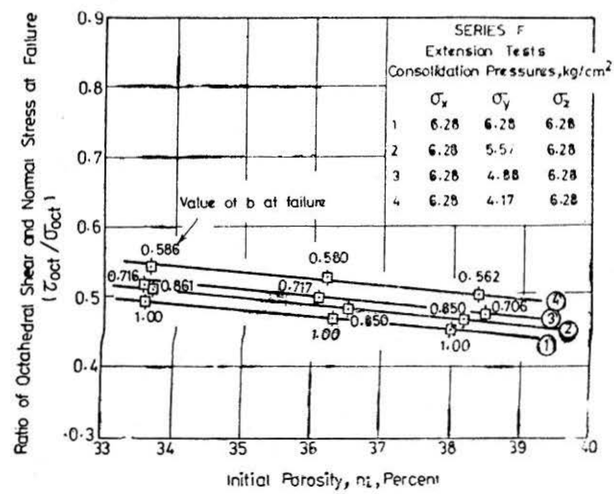

FIGURE 26 Variation of ratio of octahedral shear and octahedral normal stress at failure with initial porosity in extension tests (Series F)

compression tests in the region $b = 0$ to $b = 0.3$. In compression tests the mean curves of $(\tau_{oct}/\sigma_{oct})_f$ and $(r_{oct})_f$ relationship for different initial porosities are almost parallel to each other and the slopes of the mean curves are positive. Whereas in extension tests only one mean curve defining the relationship between the ratio $(\tau_{oct}/\sigma_{oct})_f$ and $(r_{oct})_f$ is obtained for the entire porosity range and that the slope of this line is negative

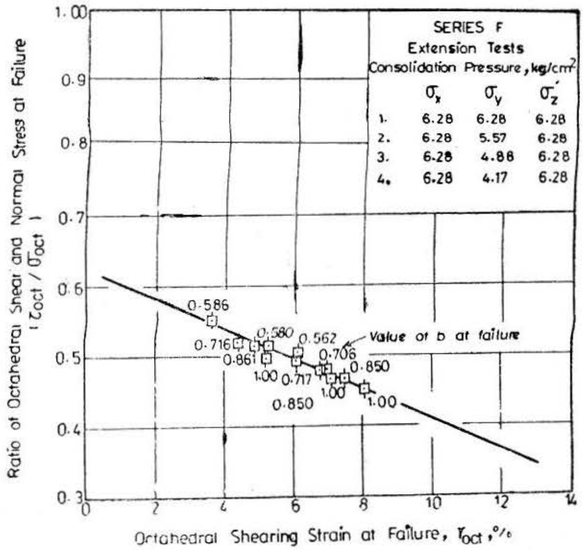

FIGURE 27 Relationship between the ratio of octahedral shear and octahedral normal stress at failure and the octahedral shearing strain at failure in extension tests (Series F)

indicating that the ratio $(\tau_{oct}/\sigma_{oct})_f$ at failure decreases as the octahedral shear strain at failure increases. This signifies the difference in stress path followed in compression (mean normal stress increasing) and extension tests (mean normal stress decreasing).

The ratio $(\tau_{oct}/\sigma_{oct})$ at failure for each test is plotted against the corresponding maximum angle of shearing resistance ϕ' in Figure 28. The corresponding values of b at failure are also labelled with the test points. The curves for values of $b = 0.0, 0.1, 0.2, 0.3$ and 0.4 are then drawn by interpolation. It is seen that in compression tests, for a given value of b at failure, a unique relationship between the ratio $(\tau_{oct}/\sigma_{oct})$ at failure and the maximum angle of shearing resistance is obtained which is independent of the stress path followed during shearing for the entire range of the initial porosities. For extension tests, irrespective of the values of b at failure, a similar relationship between the ratio $(\tau_{oct}/\sigma_{oct})_f$ and ϕ' is obtained. The mean curve from this plot seems to be almost parallel to the curve corresponding to $b = 0.4$ from the compression tests.

Conclusions

The following conclusions are drawn from this research programme:

1. The modified universal triaxial apparatus incorporates simple design features and offers independent control of the three principal stresses and measurement of the resulting principal strains. The 7.6 cm cubical soil specimen in this apparatus deforms freely without any interference from the parts of the apparatus.

2. In the case of compression tests under axisymmetric conditions, practically identical results in terms of the peak strength and the volumetric

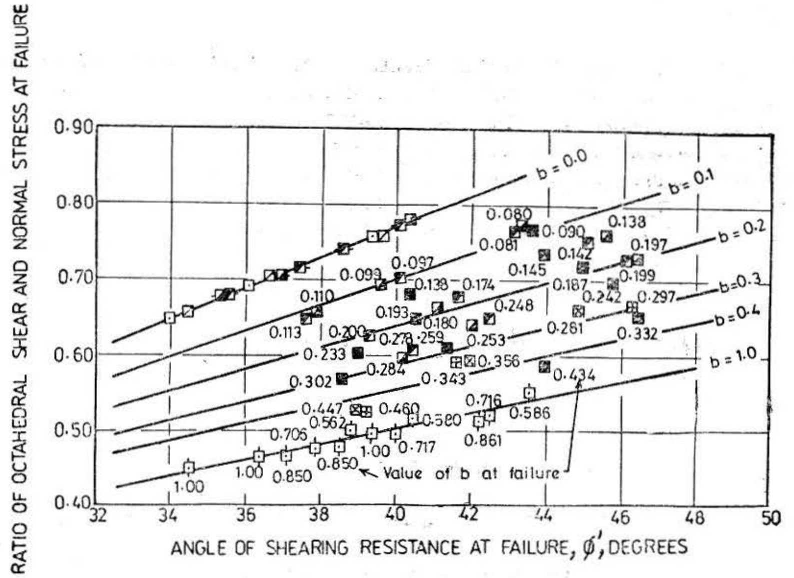

FIGURE 28 **Relationship between the ratio of octahedral shearing and octahedral normal stress at failure and the angle of shearing resistance at failure (Series A to F)**

strain rate at failure are obtained from the conventional triaxial apparatus and the universal triaxial apparatus over a complete range of initial porosities.

The steeper stress-strain curves and the lower axial strain at failure of the conventional 2:1 cylindrical sample with rough platens compared to adequately lubricated cubical sample in the universal triaxial apparatus are attributed to the difference in end conditions.

3. An approximately linear increase in the peak strength is obtained for samples of a given porosity when the intermediate principal stress increases from being equal to the minor principal stress [*i.e.*, $b = (\sigma_2' - \sigma_3')/(\sigma_1' - \sigma_3') = 0$] to the value required to maintain the conditions of plane strain and then the peak strength continually decreases to its original value at $b = 1$ ($\sigma_1' = \sigma_2'$). It is observed that the stress-strain curves, the linear strains and the volumetric strains are influenced by the stress path followed. The ratio of octahedral shear stress to octahedral normal stress at failure is found to be uniquely related to the octahedral shearing strain at failure and the maximum angle of shearing resistance, ϕ'.

4. The discontinuity in the behaviour of sand in changing over from compression to extension tests needs further investigation by conducting the tests in which the mean normal stress is continuously increasing up to $b = 1$, and the other tests in which the mean normal stress is continuously decreasing from $b = 1$ to $b \to 0$.

Acknowledgements

The authors are grateful to the Director, Indian Institute of Technology, Delhi, for providing facilities to carry out the present research programme. The first author (Rawat) gratefully acknowledges financial support in the form of research scholarship of I.I.T., Delhi. Thanks are due to the staff of Soil Mechanics Laboratory and Workshop, particularly to Messrs G.K. Mehta, T.R. Bhogal and late A.S. Bonga for their excellent work and cooperation in fabricating the universal triaxial apparatus.

Notation

The following symbols are used in this paper :

b $= (\sigma_2' - \sigma_3')/(\sigma_1' - \sigma_3')$

$\triangle V$ = change in volume of the sample

$\triangle V/V$ = volumetric strain measured from the end of consolidation

ϕ' = effective angle of shearing resistance

$\sigma_1', \sigma_2', \sigma_3'$ = major, intermediate and minor principal effective stresses respectively

$\sigma_{z'}', \sigma_{x'}', \sigma_y'$ = principal effective stresses in z, x and y directions respectively

$\sigma_{oc}{}^{t}$ = octahedral normal stress $= 1/3\left(\sigma_1' + \sigma_2' + \sigma_3'\right)$

τ_{oct} = octahedral shear stresses

$$= \tfrac{1}{3}\sqrt{\left[\left(\sigma_1' - \sigma_2'\right)^2 + \left(\sigma_2' - \sigma_3'\right)^2 + \left(\sigma_3' - \sigma_1'\right)^2\right]}$$

$\epsilon_1, \epsilon_2, \epsilon_3$ = major, intermediate and minor principal strains respectively

$\epsilon_z, \epsilon_x, \epsilon_y$ = principal strains in z, x and y direction respectively

r_{oct} = octahedral shear strain

$$= \tfrac{2}{3}\sqrt{[(\epsilon_1-\epsilon_2)^2+(\epsilon_2-\epsilon_3)^2+(\epsilon_2-\epsilon_1)^2]}$$

Subscript f denotes 'at failure'.

All strains are engineers' strain based on conditions at the end of consolidation. The volumetric strains and the volumetric strain rates were calculated from the change in burette readings. The octahedral shear strain (r_{oct}) was computed using the measured strains (ϵ_x, ϵ_y, ϵ_z) in x, y and z directions.

References

ARTHUR, J.R.F., and MENZIES, B K., (1968), Correspondence on "A New Soil Testing Apparatus", by H.Y. Ko & R.F. Scott, *Geotechnique*, Vol. 18, No. 2, pp. 271-272.

ARTHUR, J.R.F., and MENZIES, B.K., (1972), "Inherent Anisotropy in a Sand", *Geotechnique*, Vol. 22, No. 1, pp. 115-128.

BARDEN, L., and PROCTER, D.C., (1971), "The Drained Strength of Granular Material", *Canadian Geotech. Journal*, Vol. 8, No. 3, pp. 372-383.

BELL, J.M., (1965), "Stress-strain Characteristics of Cohesionless Granular Materials Subject to Statically Applied Homogeneous Loads in an Open System", *Ph. D. Thesis*, California Inst. of Tech., Pasadena Calif.

BEMBEN, S.M., (1967), "The Influence of Controlled Strain Restrains on the Strength and Behaviour During Shear of a Sand Tested with a Constant Volume", *Ph.D. Thesis*, Cornell University.

BENNET, D.H., (1969), Discussion, "Three Dimensional Stress Test" in 'New Laboratory Methods of Investigating Soil Behaviour" *Speciality Session 16. Proc. 7th Int. Conf. SMFE*, Vol. III, pp. 519-520.

BENNETT, D.H., (1971), Discussion to Session 3, "The Meaning and Measurement of Basic Soil Parameters", *Proc. Roscoe Memorial Symposium*, Cambridge, pp. 369-373.

BISHOP, A.W., (1967), Discussion to Session 3, "Shear Strength of Soil other than Clay, *Proc, Geot. Conf.*, Oslo, Vol. 2, pp. 201-204.

BISHOP, A.W., and GREEN, C.E., (1965), "The Influence of End Restraint on the Compression Strength of a Cohesionless Soil", *Geotechnique*, Vol. 15, No. 3, pp. 243-266.

BISHOP, A.W. and HENKEL, D.J., (1962), *The Measurement of Soil Properties in the Triaxial Test*, 2nd Edition, Arnold, London.

DYSON, S., (1970), "The Strength and Deformation Behaviour of a Cohesionless Soil Under Generalized Stress Conditions", *Ph.D. Thesis*, University of Aston-in-Birmingham.

ESRIG, M.I. and BEM BEN, S.M., (1965), Discussion on "Soil Properties-Shear Strength and Consolidation", *Proc. 6th Int. Conf. SMFE*, Vol. III, pp. 321-323.

GREEN, G.E., (1969), "Strength and Compressibility of Granular Materials Under Generalised Strain Conditions", *Ph.D. Thesis* (2 Vols.), London University.

GREEN, G.E., (1971*a*), "Strength and Deformation of Sand Measured in an Independent Stress Control Cell", *Proc. Roscoe Memorial Symposium*, Cambridge, pp. 285-323.

GREEN, G.E., (1971*b*), Discussion leader's closing comments, Session 3, "The Meaning and Measurement of Basic Soil Parameters", *Proc. Roscoe Memorial Symposium*, Cambridge, pp. 401-409.

GREEN, G.E., and BISHOP, A.W., (1969), "A Note on the Drained Strength of Sand Under Generalised Strain Conditions", *Geotechnique*, Vol. 19, No. 1, pp. 144-149.

GREEN, G.E., and READES, D.W., (1975), "Boundary Conditions, Anisotropy and Sample Shape Effects on the Stress-strain Behaviour of Sand in Triaxial Compression and Plane Strain", *Geotechnique*, Vol. 25, No. 2, pp. 333-356.

GUDEHUS, G., (1971), Discussion to Session 3, "The Meaning and Measurement of Basic Soil Parameters", *Proc. Roscoe Memorial Symposium*, Cambridge, pp. 373-375.

HAMBLY, E.C., (1969), "A New True Triaxial Apparatus", *Geotechnique*, Vol. 19, No. 2, pp. 307-309.

KO, H.Y., (1966), "Static Stress-Deformation Characteristics of Sand", *Ph.D. Thesis*, California Inst. of Tech., Pasadena, Calif.

KO, H.Y., and SCOTT, R.F., (1967), "A New Soil Testing Apparatus", *Geotechnique*, Vol. 17, No. 1, pp. 40-57.

KO, H.Y., and SCOTT, R.F., (1968), "Deformation of Sand at Failure", *JSMFD, ASCE*, Vol. 94, SM4, pp. 883-898.

KOLBUSZEWSKI, J.J., (1948), "An Experimental Study of the Maximum and Minimum Porosities of Sands", *Proc. 2nd Int. Conf. SMFE*, Vol. 1, pp. 158-165.

LADE, P.V., and DUNCAN, J.M., (1973), "Cubical Triaxial Tests on a Cohesionless Soil", *J. SMFD, ASCE*, Vol. 99, SM10, pp. 793-812.

LENOE, E.M., (1966), "Deformation and Failure of Granular Media Under Three Dimensional Stresses", *Experimental Mechanics*, Feb., 1966, pp. 099-104.

LEWIN, P.I., (1971), "A New Apparatus for Testing a One-Dimensionally Consolidated Clay Cube with Independent Stress Control", *Proc. Roscoe Memorial Symposium*, Cambridge, pp. 324-329.

LOMIZE, G.M., and KRYZHANOVSKY, A.L., (1967), "On the Strength of Sand", *Proc. Geot. Conf*, Oslo, Vol. 1, pp. 215-219.

LOMIZE, G.M., KRYZHANOVSKY, A.L., VORONTSOV, E.I. and GOLDIN, A.L., (1969), "Study on Deformation and Strength of Soils Under Three Dimensional State of Stresses, *Proc. 7th Int. Conf. SMFE*, Vol. I, pp. 257-265.

MALYSHEV, M.V., and FRALIS, A.D., (1968), "The Strength of Sandy Soils", (in Russian), *Proc. 3rd Budapest Conf. SMFE*, Section I, pp. 166-174.

MENZIES, B.K., (1970), "Stress Strain Anisotropy in Sands", *Ph.D. Thesis*, London University.

MENZIES, B.K., (1971), Discussion to Session 3 "The Meaning and Measurement of Basic Soil Parameters", *Proc. Roscoe Memorial Symposium*, Cambridge, pp. 368-371.

MESDARY, M.S., "The Shearing Behaviour of Granular Material Under a General Stress System", *Ph.D. Thesis*, Glasgow University.

MESDARY, M.S., and SUTHERLAND, H.B., (1970), Correspondence on "A Note on the Drained Strength of Sand Under Generalised Strain Condition", by G.E. Green and A.W. Bishop, *Geotechnique*, Vol. 20, No. 2, pp. 210-212.

PEARCE, J.A., (1971), "A New True Triaxial Apparatus", *Proc. Roscoe Memorial Symposium*, Cambridge, pp. 330-339.

PROCTER, D.C., and BARDEN, L., (1969), Correspondence on "A Note on the Drained Strength of Sand Under Generalized Strain Conditions" by G.E. Green and A.W. Bishop, *Geotechnique*, Vol. 19, No. 3, pp. 421-426.

RAMAMURTHY, T., (1970), "A Universal Triaxial Apparatus", *J. Indian Nat. Soc. SMFE*, Vol. 9, No. 3, pp. 251-269.

RAMAMURTHY, T. and RAWAT, P.C., (1971), Discussion on "Comparison of Plane Strain and Triaxial Tests on Sand" by K.L. Lee, *JSMFD, ASCE*, Vol. 97, SM2, pp. 489-497.

RAMAMURTHY, T., and RAWAT, P.C., (1973), "Shear Strength of Sand Under General Stress System", *Proc. 8th Int. Conf. SMFE*, Vol. I, pp. 339-342.

RAWAT, P.C., (1976), "Shear Behaviour of Cohesionless Materials Under Generalised Conditions of Stress and Strain", *Ph.D. Thesis*, Indian Institute of Technology, Delhi.

READES, D.W., (1972), "Stress-Strain Characteristics of a Sand Under Three Dimensional Loading", *Ph.D. Thesis*, University of London.

READES, D.W., and GREEN, G.E., (1976), "Independent Stress Control and Triaxial Extension Tests on Sand", *Geotechnique*, Vol. 26, No. 4, pp. 551-576.

SHIBATA, T., and KARUBE, D., (1965), "Influence of the Variation of the Intermediate Principal Stress on the Mechanical Properties of Normally Consolidated Clays", *Proc. 6th Int. Conf. SMFE*, Vol. I, pp. 359-363.

SMITH, I.M., and KAY, S., (1971), "Stress Analysis of Contractive or Dilative Soil", *JSMFD, ASCE*, Vol. 97, SM7, pp. 981-997.

SOMASHEKAR, B.V., (1977), "Studies on Stress Deformation and Strength of Soils Under General Stress State", *Ph D. Thesis*, Indian Institute of Science, Bangalore.

SUTHERLAND, H.B., (1971), Discussion to Session 3 "The Meaning and Measurement of Basic Soil Parameters", *Proc. Rorcoe Memorial Symposium*, Cambridge, pp. 376-377.

SUTHERLAND, H.B., and MESDARY, M.S., (1969), "The Influence of the Intermediate Principal Stress on the Strength of Sand", *Proc. 7th Int. Conf. SMFE*, Vol. I, pp. 391-399.

YONG, R.N., and McKYES, E., (1967), "Yielding of Clay in a Complex Stress Field", *Proc. 3rd Pan Am. Conf. SMFE*, Vol. I.

YONG, R.M., and McKYES, E., (1971), "Yield and Failure of a Clay Under Triaxial Stresses", *JSMFD, ASCE*, Vol. 97, SM1, pp. 159-176.